doi: 10.1038/nature06350

Coevolution with viruses drives the evolution of bacterial mutation rates

Csaba Pal[1], María D. Maciá[2], Antonio Oliver[2], Ira Schachar[1] & Angus Buckling[1]

[1]*Department of Zoology, University of Oxford, Oxford OX1 3PS, UK*

[2]*Servicio de Microbiologia and Unidad de Investigación, Hospital Son Dureta, Instituto Universitario de Investigación en Ciencias de la Salud (IUNICS) 07014, Palma de Mallorca, Spain.*

Simulation of mutator dynamics under host parasite coevolution

The robustness of the verbal model was strengthened by theoretical simulations, derived by combinations of previous multi-locus models of host-parasite coevolution[1] and mutator dynamics[2, 3]. The model is not intended to be a complete representation of the experimental system. Rather, the main goal is to identify how sensitive the prediction that coevolution can drive the evolution of mutators is to variation in parameter values.

The model assumes that both the host and the parasite are haploid, reproduce asexually, and have reasonably large population sizes (N_H and N_P). Most simulations were carried out under the simplifying assumption that population size remains constant during the coevolutionary process (soft-selection). However, in reality, the extent of phage (and bacterial) propagations and hence population sizes of coevolving partners may strongly depend on bacterial resistance and phage infectivity. For example, phage particles often propagate in bursts under permissive conditions (e.g. when hosts are sensitive), leading to large variation in phage densities. The impact of resistance to phages on host population size (hard-selection), was incorporated by the following equation:

$$N_H(t+1) = N_{\min} + N_{\max}\left(W_{H,t}\right)^{\beta},$$

where $N_H(t+1)$ denotes host population size at timepoint $t+1$, N_{min} and N_{max} denote host population sizes when resistance is minimal and maximal, respectively. $W_{H,t}$ ($0 \le W_{H,t} \le 1$) is the host population fitness, which is a function of resistance, at timepoint t, while the scaling factor β determines the extent of dependence of population size on resistance. When, $\beta=0$, population size equals $N_{min} + N_{max}$, and it remains constant throughout the simulations. With growing β, the

impact of resistance on population size increases exponentially. Analogous equations describe parasite population size variation. Note, that while the link between changes in resistance and bacterial population size is unclear, the 'drastic' exponential scaling between the two variables is likely to overestimate the strength of the relationship. Based on experimental data[4], we assumed that bacterial population size is roughly 100-fold higher than phage population size. Relative mutation rates are expected to show the opposite pattern[5,6] (see below).

The genetics of host resistance and parasite infectivity is governed by two biallelic loci, which yields four potential genotypes for the host (*H00, H01, H10, H11*) and the parasite (*P00, P01, P10, P11*). The fitness of interacting host and parasite genotypes follow the treatment of Agrawal & Lively[1] (Supplementary Table 1). Briefly, the probability of successful parasite invasion (host resistance) is governed by several parameters. Parameter *a* specifies the *type* and *specificity* of interaction. When $a=0$ the interaction follows the rules of a matching allele model (MAM). In this case, infection requires a perfect match between host and parasite genotypes. When $a=1$, the models follows a gene-for-gene model (GFGM). The key feature of the GFGM is that parasite (hosts) can acquire a broader range of infectivity (resistance). Patterns of local adaptation in this system suggest *a* falls between these two extremes in our system[7], but note that the specificity appears to be pure GFGM in the well studied *Eschirichia coli* – lytic bacteriophage systems[8]. Parameter *c* (or *k* in the parasite) measures the intrinsic costs associated with resistance (infectivity) alleles. The simulated host genome also has one mutator locus (with a non-mutator or mutator allele) and 10 viability loci that could carry either wild type or deleterious allele. This creates a cost to mutator genotypes because there is a higher probability of each viability locus having a deleterious allele. We assume that individual deleterious mutations at host viability loci act independently, and carrying deleterious mutations at these loci has effect on fitness but not on the effect on invasion probability of the parasite (only alleles at resistance loci matter). Note, that

as the model concentrates on the evolutionary dynamics of host mutator genotypes, parasite viability loci that can carry deleterious alleles can be safely ignored.

The probabilities of different mutation events are specified by Supplementary Table 2. At start of the simulations, host population was set to be sensitive to the parasite and carried no deleterious alleles at viability loci. For more details on parameter set used, see Supplementary Table 2. In general, the fitness (or payoff) of a host with resistance genotype *i* when infected by parasite *j* is:

$$P_H(i, j) = (1 - a \cdot c)^z (1 - s \cdot W_{Pji}),$$

where, *s* is the maximum virulence of a parasite, *c* is the cost of carrying a resistance allele, *z* is the number of resistance alleles carried by the host, and W_{Pji} is the fitness (payoff) of parasite *j* on host *i.* The expected fitness of host genotype with resistance genotype *i* and *n* number of deleterious mutations is:

$$W_H(i, n) = (1 - s_v)^n \sum_{j=1}^{4} P_H(i, j) \cdot y_j ,$$

where the s_v defines the impact of individual deleterious mutations at viability loci, and y_j is the frequency parasite genotype *j.* Similarly, the expected fitness of parasite *j* is:

$$W_P(j) = \sum_{i=1}^{4} W_{Pji} x_i ,$$

where x_i denotes the frequency of host genotype *i.* Each generation consists of selection, mutation, and random sampling. The host (parasite) can change their alleles at resistance (infectivity), viability and mutator loci by random mutation; at the start of each simulation, the whole host (parasite) population was isogenic at their resistance (infectivity) and viability loci.

Mutations occurred at constant rates per replication: in the mutator genotype, mutation rates were increased 100-fold at all loci. Selection and mutations events acting on host and parasite genotypes were described by a standard set of difference equations. Genotypes present at a frequency of less than 1 in 1000 were sampled with a Poisson sampling procedure, whereas the sample sizes of more common genotypes were deterministic. 100 independent simulations were done for each parameter set.

The initial frequency of the host mutator allele was generally set to 10^{-3}, and we followed its frequency for 2000 generations. Under some conditions (e.g. when the specificity of host-parasite interaction is low), mutators can increase in frequency during the course of evolution, but they do not become fixed in the population. Rather, they follow the oscillation of host resistance genotypes (Supplementary figure 1). We therefore report the frequency of mutator alleles averaged over the last 500 generations of each simulation. As mutation events affect mutator locus themselves, fixation events were considered to be those when at least 99% of the population carried the mutator allele.

While several genetic and ecological parameters have some influence, mutator alleles can spread under wide range of conditions. Reduced specificity of host-parasite interactions (i.e. more GFGM-like; a increases) generally slows down co-evolutionary dynamics, leading to a reduction in the spread of mutator alleles in the population (Supplementary figure 2a). Both high costs of bacterial resistance (Supplementary figure 2b) and increased deleterious mutational load (data not shown) cause an overall reduction in mutator frequency.

The results presented so far were based on a soft-selection model that assumes constant population size during the course of evolution ($\beta=0$). We briefly examined how departure from

constant population size modifies the spread of mutator alleles. Population size variation across time (and hence reduced average effective population size) can have a complex impact on the spread of mutators, as it may affect both co-evolutionary dynamics, the waiting time for new beneficial mutations, and the net selective advantage of mutator alleles. We observed a gradual decline in the frequency of mutators with increasing β under wide range of parameter sets (for an example, see Supplementary figure 2c). However, our simulations also suggest that the co-evolutionary dynamics (and hence the spread of mutators) is rather insensitive to details of host-parasite population dynamics. For example, when β =15, a 30% decrease in bacterial resistance yields greater than 500 fold-decrease in bacterial population size, but less than 4 fold difference in the average frequency of mutators at the end of simulations. Similar results hold when population size variation was restricted to the host (data not shown).

The impact of starting frequency of mutators was more complex. For mutators to hitch-hike to high frequency, they must become linked with beneficial mutations, and if mutators are at a very low frequency in the population, the probability of this happening before beneficial mutations occur in the higher frequency wildtype genetic background is decreased[2,3,8]. As such, the probability of mutators increasing in frequency is positive-frequency dependent. In our simulations, under conditions where wild type can mutate to mutators (and vice versa), changing the starting frequency of mutators had a negligible effect on their spread in the population (Supplementary figure 2d). However, this is because an equilibrium frequency of mutators will always be reached as a result of a mutation-selection balance. We altered our simulations by preventing wildtype mutating to mutators (and vice versa), hence simulating the invasion dynamics of a single mutator allele, and found that the invasion success of mutators was indeed positive frequency dependent (Supplementary figure 2e). In other words, the higher initial frequency of mutators at start of the simulations, the more likely they can spread in the

populations. This increase goes far beyond what one would expect in the case of a neutral allele, and hence is governed by positive frequency dependent selection. Previous theoretical work suggests other mechanisms by which mutators are able to invade. First, if multiple mutations are required for the beneficial phenotype: a 100-fold higher mutation rate would result in a 10000-fold (100 x 100) increase in the rate of acquisition of two beneficial mutations in the same genome[3]. Second, if the resistance mutation reaches a higher frequency in the mutator sub-population relative to the wild type sub-population, resulting in a higher mean fitness of mutators relative to wildtypes[9]

Isolation of phage

To isolate phage from bacteria, 100ml of chloroform was added to 900ml of culture and then centrifuged at 13,000 rpm. for 3 min[4]. This procedure lyses and pellets the bacterial cells to the bottom of the tubes, leaving a suspension of phages in the supernatant. The phage samples were stored at 4 C, and their density elucidated by plating onto soft agar plates containing exponentially growing *P. fluorescens* SBW25[4].

Measuring coevolution

We confirmed results from previous studies that phages repeatedly evolved increased infectivity to their contemporary bacterial populations, and hence imposed selection for novel bacterial resistance mechanisms. Four replicate populations were randomly chosen from those in which both bacteria and phages remained at detectable levels for the duration of the experiment. Assuming phages evolve increased infectivity to the bacterial populations they interact with, phage from a few generations in the future should be better at infecting contemporary bacteria than phages from a few generations in the past. Infectivity of phage populations to a given bacterial population was determined by their ability to inhibit bacterial growth. Approximately

1000 bacterial cells from each bacterial population were inoculated in duplicate (for each phage population that the bacterial population was to be tested against) into individual microtitre plate wells containing 180 μl KB, and 20 μl samples of a phage population added to one well, and 20 μl of KB added to the other. Cultures were grown for 24 hours at 28C. Bacterial growth inhibition (phage infectivity) was measured by the ratio of final cell densities in the presence and absence of a given viral population, as determined from the optical densities of cultures at 600nm. Note that bacterial populations were never driven extinct by phages in these assays. We confirmed the reliability of this method by streaking independent bacterial colonies across a perpendicular line of phage streaked on a KB agar plate, as done in previous studies[4,7] (data not shown).

The persistent evolution of phage infectivity was inferred from the negative relationship between phage infectivity and time point from which phages were isolated (past, contemporary and future) for bacteria isolated at multiple time points (transfers 6, 12 and 18) (Supplementary figure 3a; 12 out of 12 relationships were negative; Sign test: $P < 0.01$). Crucially, there was no evidence that the mean infectivity of past, contemporary, and future phage populations to each of contemporary bacterial populations ($n = 12$) showed any consistent change through time (Spearman rank correlation; $P > 0.2$). This demonstrates that the bacteria must be evolving resistance in response to changes in infectivity; i.e. the bacteria and phages coevolved.

We also determined if resistance and infectivity ranges increased relative to the ancestral bacteria and phage, as has been observed in previous studies. We tested the resistance of 28 evolved and the ancestral bacterial populations against 21 evolved phage populations (those that had not gone extinct by the end of the experiment) and the ancestral phage population, in every possible combination. Resistance (infectivity) was determined as above (Supplementary figure 3b).

Evolved bacterial populations have higher resistance against ancestral phage population compared to their mean resistance against the 21 evolved phage populations (Wilcoxon-Matched Pairs test N = 28, Z = 4.62, $P < 10\text{-}5$), providing evidence that evolved phage populations have acquired broader range of infectivity. Evolved phage populations have much higher infectivity to ancestral bacterial populations compared to the mean infectivity against evolved bacterial populations (Wilcoxon-Matched Pairs test N = 21, Z = 3.91, $P < 10\text{-}4$). This result suggests that evolved bacterial populations also acquired a broader resistance range. There was no significant difference in infectivity between evolved and ancestral phage on ancestral bacteria.

Complementation of mutator clones with wildtype MMR genes

The plasmids containing the *P. aeruginosa* PA01 wildtype MMR genes *mutS* (pUCPMS) and *mutL* (pJMML) were introduced into the *P. fluorescens* mutator clones and the wildtype SBW25 strain by electroporation[10,11]. The sequences of *mutS* and *mutL* genes of *P. aeruginosa* are very similar to their respective orthologs in *P. fluorescens* (81% and 84% amino acid identities). Plasmid pUCP24 (cloning vector) was electroporated into the same strains as a control. Transformants were selected in Luria-Bertani (LB) agar plates containing 30 μg/ml of gentamicin (pUCPMS or pUCP24) or 100 μg/ml of kanamycin (pJMML). To evaluate the complementation of the mutator phenotypes with the wildtype MMR genes, mutation frequencies to rifampicin (100 μg/ml) resistance were determined in parallel for the original strains as well as for those same producing pUCP24, pUCPMS, or pJMML (Supplementary table 3).

Phage extinction and mutator dynamics

The following procedure was used to see if there was any relationship between phage 'extinction' (density below the detection threshold of approximately 200 phages per culture), and the presence or absence of evolved mutator bacteria. We identified four independent events:

extinction/persistence of phage population at transfer T+6 in the presence of mutator/non-mutator bacterial populations at transfer T (T: 6,12,18). These events were counted across the 36 evolved bacterial-phage populations and 3 timepoints, leading to four numbers: $N_{M,E}$, $N_{M,P}$, $N_{NM,E}$ and $N_{NM,P}$, where M and NM denote mutator/non-mutator population at time point T, while P and E denote persistence/extinction of phage population from T to T+6, respectively (The procedure has the desired effect of excluding all events where the populations have no phage at time point T). Under the assumption that phage populations are especially likely to get extinct in the presence of bacterial mutator populations, the ratio $R = \frac{N_{M,E}/(N_{M,E}+N_{M,P})}{N_{NM,E}/(N_{NM,E}+N_{NM,P})}$) is expected to be higher than chance. To investigate any significant departure from random expectations, we randomly assigned which bacterial populations are mutators (but conserved the number and history of mutator populations across timepoints), and then R was recalculated. This procedure was repeated 10^4 times. Crucially, our protocol controls for potential errors due to biased experimental starting conditions (i.e. presence of the virus and non-mutator ancestral bacterial populations). The *P*-value was estimated by calculating the fraction of cases where the original R was higher than R derived from randomizations. Note that once a phage population reached undetectable levels, they were never subsequently detected at later time points.

Construction of *P. fluorescens* SBW25 *mutS* knock out mutants

An SBW25 *mutS* knock out mutant was constructed following the procedure previously described[12] for gene deletion and antibiotic marker recycling. Upstream and downstream PCR products (Supplementary table 4) of *mutS* were cloned by a three way ligation into pEX100Tlink (deleted for the HindIII site) to obtain plasmid pEXTpfmS that was transformed into *E. coli* XL_1Blue strain. Transformants were selected in 30 μg/ml ampicillin MacConkey agar plates. The *lox* flanked gentamicin resistance cassette (*aac1*) obtained by HindIII restriction of plasmid

pUCGm*lox* was cloned into the single site for this enzyme formed by the ligation between the two flanking fragments, producing plasmid pEXTpfmSGm that was transformed into *E. coli* XL_1Blue strain. Transformants were selected in 30 μg/ml ampicillin-10 μg/ml gentamicin LB agar plates. These plasmids were then transformed into the *E. coli* S17-1 helper strain. The SBW25 *mutS* (SBW25mSGm) mutant was generated by introducing pEXTpfmSGm from *E. coli* S17-1 by conjugation and selecting for double recombinants using 5% sucrose-5 μg/ml gentamicin-1 μg/ml cefotaxime LB agar plates. Double recombinants were checked by PCR amplification. To generate the knock out mutant without the gentamicin resistance marker (SBW25mS), plasmid pCM157 was introduced by electroporation into SBW25mSGm and transformants were selected in 10 μg/ml tetracycline LB agar plates. One transformant was grown overnight in 10 μg/ml tetracycline LB broth in order to allow the expression of the *cre* recombinase. Plasmid pCM157 was then cured from the strains by two successive passages on LB broth. Finally, the knock out was checked by PCR amplification and sequencing to ascertain that the corresponding genes were properly disrupted. Complementation of the strain without the gentamicin resistance marker was carried out as described above, as a control (Supplementary table 3).

Comparison of wildtype and isogenic mutator bacteria

To further test whether increased mutation rates contribute to faster adaptation to phage, we constructed an isogenic mutant of *P. fluorescens* SBW25 with a *mutS* deletion, which conferred a 100-fold higher mutation rate. Competition experiments were performed between the wild type and *mutS* knockout (Figure 4). Approximately 10^8 cells of mutator and wild type bacteria at $1{:}10^2$, $1{:}\ 10^4$ and $1{:}10^6$ ratio to KB microcosms were inoculated into 6 cultures at each ratio. Each culture was then inoculated with 10^5 clonal particles of phage SBW25Φ2. Six control replicates (at $1{:}10^2$) were established that contained no phage. Cultures were propagated in a

shaken incubator (200rpm) at 28C. Sixty microlitres of each culture was transferred to fresh medium every day, for 6 transfers. After every second transfer, densities of mutator and wild type bacteria were estimated by plating diluted cultures on non-selective (KB) and selective (KB +10 μl/ml gentamicin) solid media. Only the mutator strain was able to grow on the gentamicin plates. To further investigate phage extinction probabilities, we inoculated 48 microcosms with 10^8 bacterial cells and 10^5 phage; half of the microcosms were inoculated with wildtype cells only, and half with the *mutS* knockout cells only. We propagated cultures for 12 transfers, as above, after which we estimated phage densities. Note that the shorter time scale of the experiments using the *mutS* knockout compared with the previous experiment was chosen to minimise the effect of wildtype populations evolving elevated mutation rates.

References

1. Agrawal, A. F. & Lively, C. M. Infection genetics: gene-for-gene versus matching-alleles models and all points in between. *Evol. Ecol Res.* **4**, 79-90 (2002).
2. Tenaillon, O., Le Nagard, H., Godelle, B. & Taddei, F. Mutators and sex in bacteria: conflict between adaptive strategies. *Proc. Natl Acad. Sci. USA* **97**, 10465-70 (2000).
3. Tenaillon, O., Toupance, B., Le Nagard, H., Taddei, F. & Godelle, B. Mutators, population size, adaptive landscape and the adaptation of asexual populations of bacteria. *Genetics* **152**, 485-93 (1999).
4. Buckling, A. & Rainey, P. B. Antagonistic coevolution between a bacterium and a bacteriophage. *Proc. R. Soc. Lond. B* **269,** 931-936 (2002).
5. Drake, J. W. A constant rate of spontaneous mutation in DNA-based microbes. *Proc. Natl Acad. Sci. USA* **88**, 7160-4 (1991).

6. Malpica, J. M. et al. The rate and character of spontaneous mutation in an RNA virus. *Genetics* **162**, 1505-11 (2002).

7. Morgan, A. D., Gandon, S. & Buckling, A. The effect of migration on local adaptation in a coevolving host-parasite system. *Nature* **437**, 253-256 (2005).

8. Lenski, R. E. & Levin, B. R. Constraints on the coevolution of bacteria and virulent phage: A model, some experiments, and predictions for natural communities. *Am. Nat.* **125**, 585-602 (1985).

9. Tanaka, M. M., Bergstrom, C. T. & Levin, B. R. The evolution of mutator genes in bacterial populations: The roles of environmental change and timing. *Genetics* **164**, 843-854 (2003).

10. Oliver, A., Levin, B. R., Juan, C., Baquero, F. & Blazquez, J. Hypermutation and the preexistence of antibiotic-resistant *Pseudomonas aeruginosa* mutants: Implications for susceptibility testing and treatment of chronic infections. *Antimicrob. Agents Chemother.* **48**, 4226-4233 (2004).

11. Oliver, A., Baquero, F. & Blazquez, J. The mismatch repair system (mutS, mutL and uvrD genes) in *Pseudomonas aeruginosa*: molecular characterization of naturally occurring mutants. *Mol. Microbiol.* **43**, 1641-1650 (2002).

12. Quénée, L., Lamotte, D., & Polack, B. Combined *sacB*-based negative selection and cre-lox antibiotic marker recycling for efficient gene deletion in *Pseudomonas aeruginosa*. *BioTechniques* **38**, 63-67 (2005).

Supplementary table 1. Fitness matrices of interacting host and parasite genotypes (from reference 1). Table 1a shows parasite fitness of genotype *j* on host genotype *i* (W_{Pji}). Parameter *k* measures the cost of increased infectivity. Table 1b show host fitness.

		Host (i)			
		H00 (i=1)	H01 (i=2)	H10 (i=3)	H11 (i=4)
Parasite (j)	P00 (j=1)	1	0	0	0
	P01 (j=2)	$a(1-ak)$	$1-ak$	0	0
	P10 (j=3)	$a(1-ak)$	0	$1-ak$	0
	P11 (j=4)	$a^2(1-ak)^2$	$a(1-ak)^2$	$a(1-ak)^2$	$(1-ak)^2$

Table 1a.

		Host (i)			
		H00	H01	H10	H11
Parasite (j)	P00	$1-s$	$1-ac$	$1-ac$	$(1-ac)^2$
	P01	$1-sa(1-ak)$	$1-ac(1-s(1-ak))$	$1-ac$	$(1-ac)^2$
	P10	$1-sa(1-ak)$	$1-ac$	$1-ac(1-s(1-ak))$	$(1-ac)^2$
	P11	$1-sa^2(1-ak)^2$	$1-ac(1-s(1-ak)^2)$	$1-ac(1-s(1-ak)^2)$	$(1-ac)^2(1-s(1-ak)^2)$

Table 1b

Supplementary Table 2. Parameter set used in this study. Unless otherwise indicated in the figure legends, these parameter values were used during the simulations.

Parameter	Symbol	Value used in the simulations
Population size (parasite)	N_P	10^4
Population size (host)	N_H	10^6
Mutation rate at host resistance loci	μ_H	10^{-6}
Rate of deleterious mutations at host viability loci	μ_H	10^{-6}
Impact of individual deleterious mutations at individual viability locus	s_v	10^{-2}
Number of viability loci	-	10
Mutation rate from non-mutator to mutator (and vice versa)	-	10^{-6} (10^{-8})
Mutation rate at parasite virulence loci	μ_P	10^{-4}
Maximal impact of the virus on host fitness	s	0.3
Cost of resistance (host)	c	10^{-2} (but see Supplementary figure 2c)
Cost of virulence (parasite)	k	10^{-2}
Impact of host resistance/viral infectivity on population size	β	0 (but see Supplementary figure 2d)

Supplementary Table 3. Results for complementation experiments of mutator clones with wild-type MMR genes. Mutation frequencies to rifampicin (100 μg/mL) resistance. Positive complementation results (Ca. 2 Log drecrease in the mutation frequency when producing the plasmids pUCPMS or pJMML) are shown in bold.

Strain	Mutation frequency when producing the plasmid[a]			
	None	**pUCP24**	**pUCPMS**	**pJMML**
SBW25	$5X10^{-9}$	$7X10^{-9}$	$8X10^{-9}$	$5X10^{-9}$
SBW25*mS*	$5X10^{-6}$	$7X10^{-6}$	**$7X10^{-8}$**	$6X10^{-6}$
P1C1	$1X10^{-5}$	$2X10^{-5}$	**$9X10^{-8}$**	$1X10^{-5}$
P2C1	$7X10^{-6}$	$3X10^{-6}$	$4X10^{-6}$	**$1X10^{-8}$**
P3C1	$4X10^{-6}$	$4X10^{-6}$	$8X10^{-6}$	**$3X10^{-8}$**
P4C1	$5X10^{-6}$	$1X10^{-5}$	$8X10^{-6}$	**$3X10^{-8}$**
P5C1	$4X10^{-6}$	$5X10^{-6}$	$1X10^{-6}$	**$7X10^{-9}$**
P6C1	$6X10^{-6}$	$4X10^{-6}$	$8X10^{-6}$	**$2X10^{-8}$**
P7C1	$1X10^{-5}$	$2X10^{-5}$	$1X10^{-5}$	$1X10^{-5}$

Supplementary Table 4. Primers used for the construction of *P. fluorescens* SBW25 *mutS* knock out mutants.

Primer	Sequence (5`-3`)[a]	PCR product size (bp)
mutSpf-ERF1	TCGAATTCAGCCTGCTCCCCACCTCT	557
mutSpf-HDR1	TCAAGCTTAGGTTATCGCGACGCTCGT	
mutSpf-HDF2	TCAAGCTTCTATGCCAGCAGTTCTCGGTG	649
mutSpf-BHR2	TCGGATCCTCTTGAGTACGCCGCCGTC	

[a] Sites for restriction endonucleases are underlined

Figure legends

Supplementary figure 1. Examples of coevolutionary dynamics and evolution of mutators. Both figures show the frequency of one host resistance genotype and the mutator allele as a function of time. (a) When the specificity of host-parasite interactions was low (a=0.9), the mutator allele spread in the populations, but its frequency oscillated. (b) When host population size is very low, coevolutionary dynamics became very slow. In this case, mutators often failed to spread. Parameter values: a) $N\mu = 10^{-1}$, a=0.9. b) $N\mu = 10^{-3}$, a=0.9. $N\mu$ indicates the product of host mutation rate and host population size. For another other example, see Figure 1 in the main text.

Supplementary figure 2. Impact of genetic and ecological variables on the spread of host mutators after 200 generations coevolving with parasites. All figures show the results of 100 independent runs under each parameter sets. The figures show the average frequency of mutators (very similar results hold for the frequency of populations in which mutators were fixed). (a) The frequency of mutators declines with decreasing host-parasite interaction specificities, i.e. as the interaction becomes more GFGM-like (increasing a). b) Increasing the cost of bacterial resistance causes a decline in average mutator frequency. Under the parameter values studied, this effect is however weak: a 100-fold increase in costs causes little more than 2 fold difference in mutator frequency. c) Large fluctuations in the sizes of host and/or parasite populations ($\beta >> 0$) causes a decline in the frequency of mutators. d) The frequency of the mutator allele at the start of the simulations has little impact on its spread, as long as population size is relatively high and the wildtype can mutate to mutators. e) Decreasing the frequency of the mutator allele at the start of the simulations decreases its spread if wild type is unable to mutate to mutators. All figures show mean±2SEM. Parameter values: a) $N\mu = 1$, a=0; b) $N\mu = 10^{-1}$; c) $N\mu$=1 a=0.9; d) $N\mu = -1$, a=0.

Supplementary figure 3. Bacteria-phage coevolution. Data shows the ratio of final population sizes of a given bacterial population in the presence versus absence of focal phage populations (a proxy of bacterial resistance). a) Resistance of 4 bacterial populations at 3 time points (transfer 6, 12 and 18) to phage from 6 transfers in the past (left point on each line), contemporary phage (middle point) and 6 transfers in the future (right point). Continual evolution of phage infectivity is shown by the increase in infectivity from past to future phage populations. b) Resistance of evolved and ancestral bacteria to evolved an ancestral phage. Bars show mean±2SEM. Evolved bacteria and phage have broader resistance and infectivity ranges, respectively.

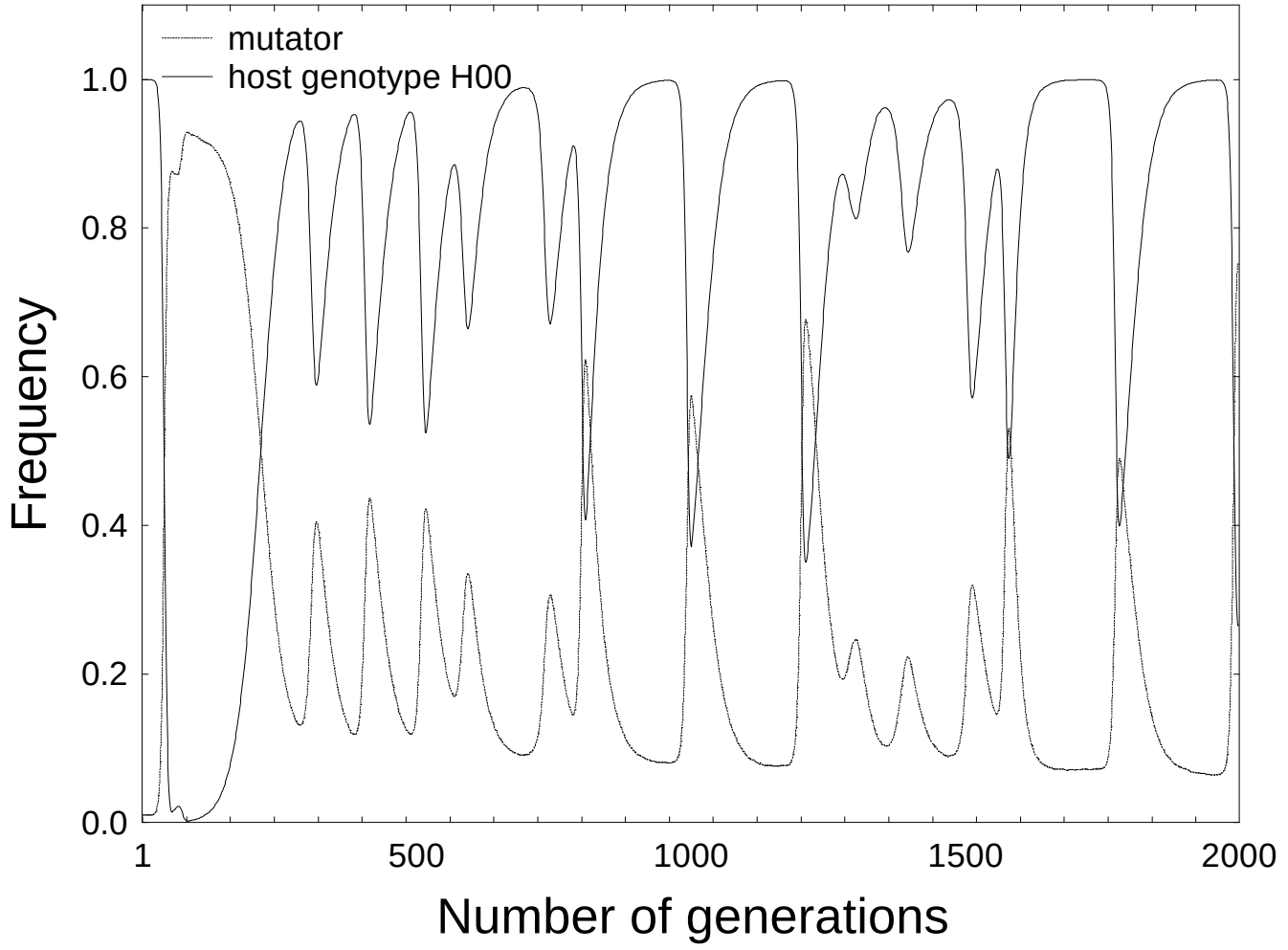

Supplementary figure 1a

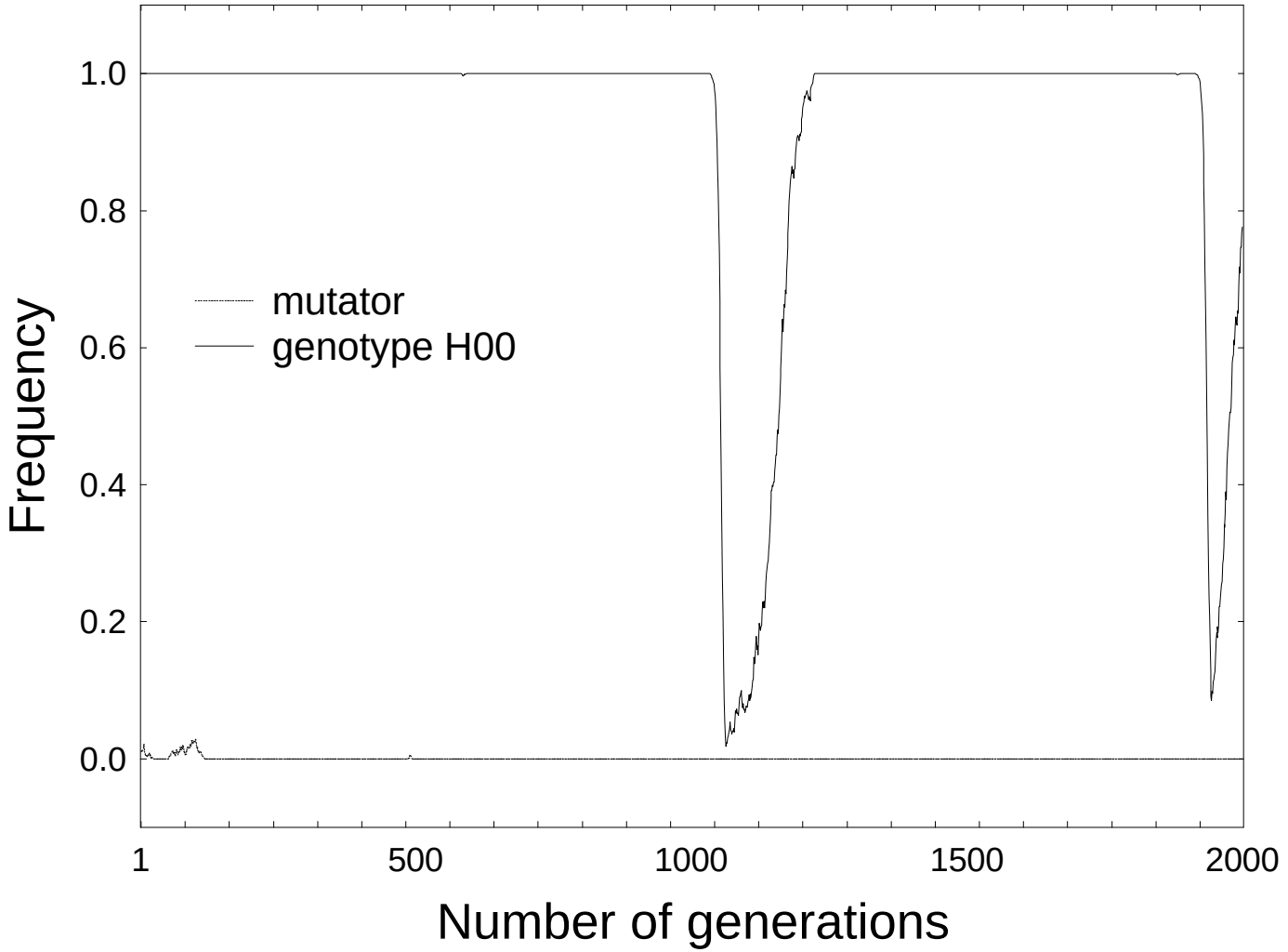

Supplementary figure 1b

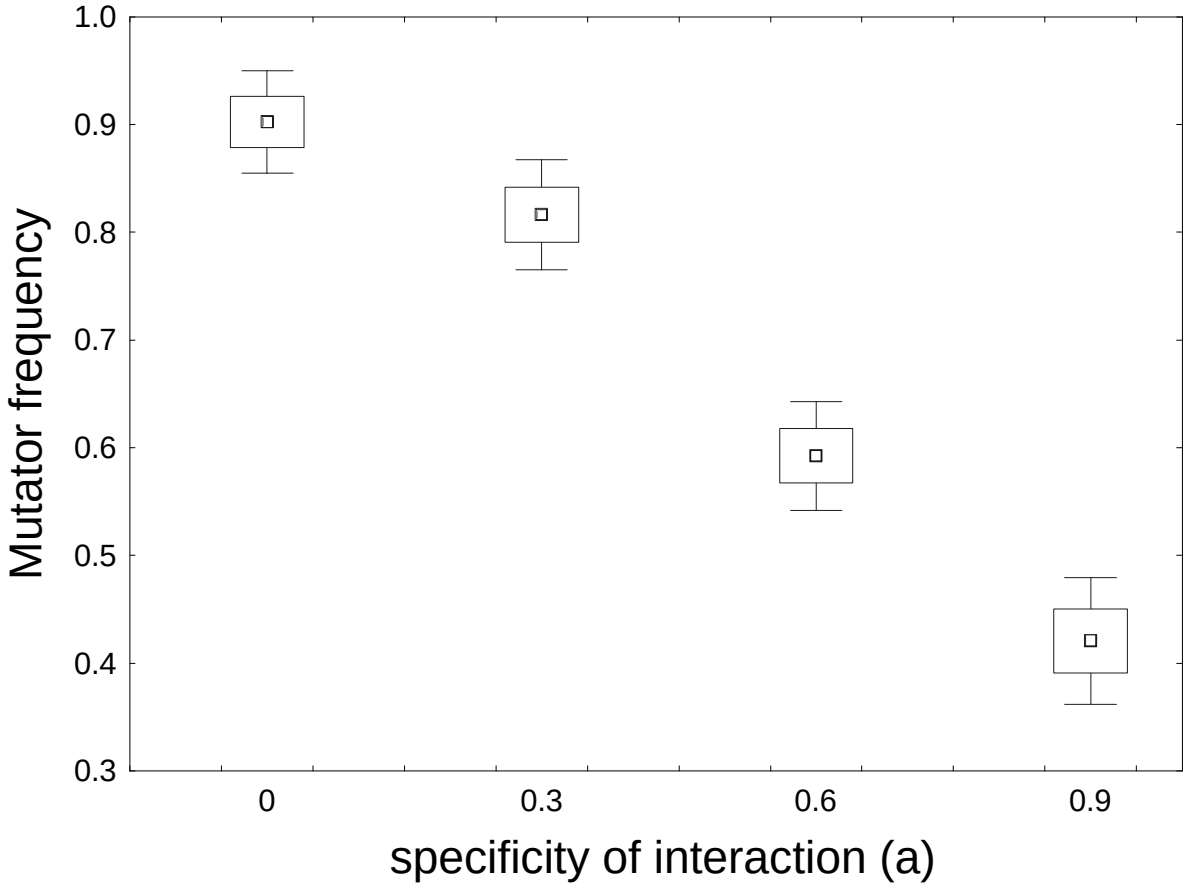

Supplementary figure 2a

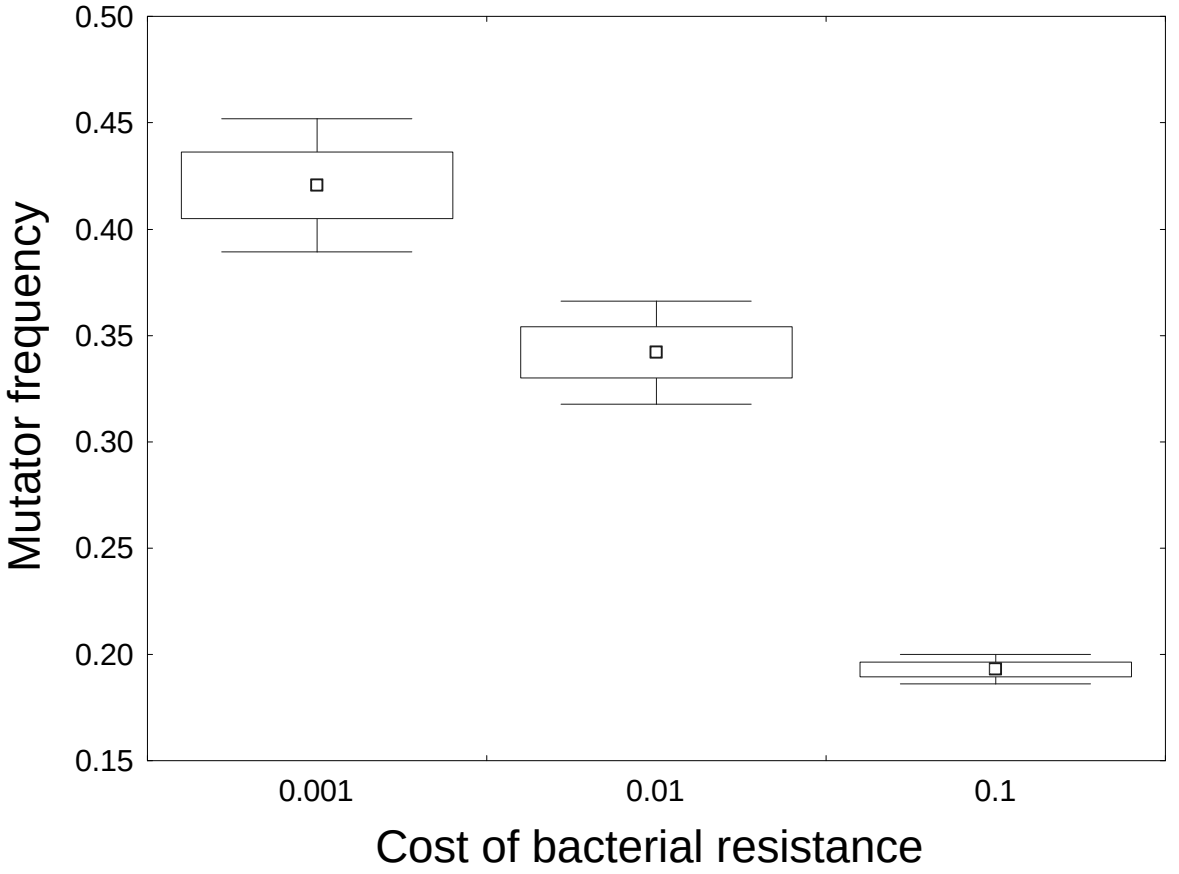

Supplementary figure 2b

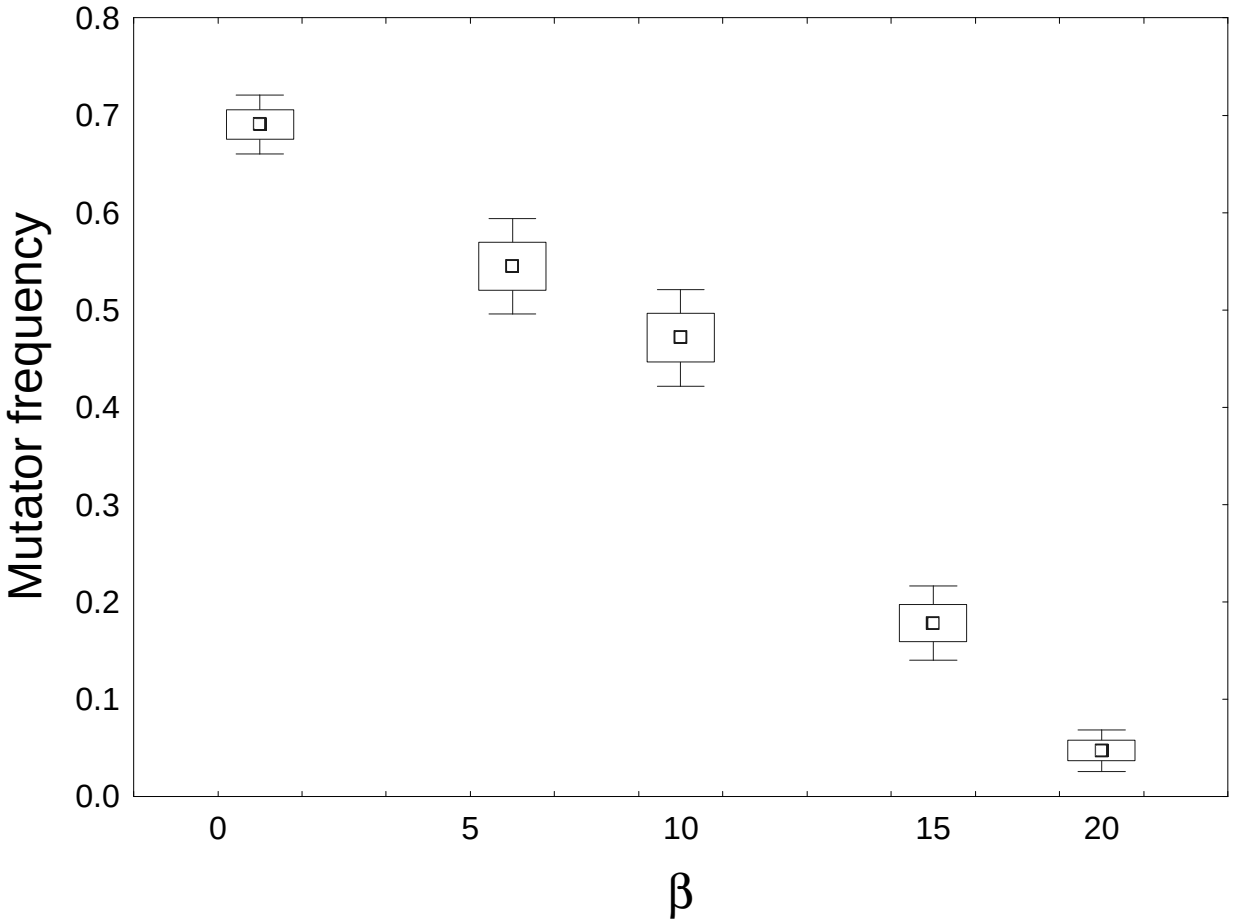

Supplementary figure 2c

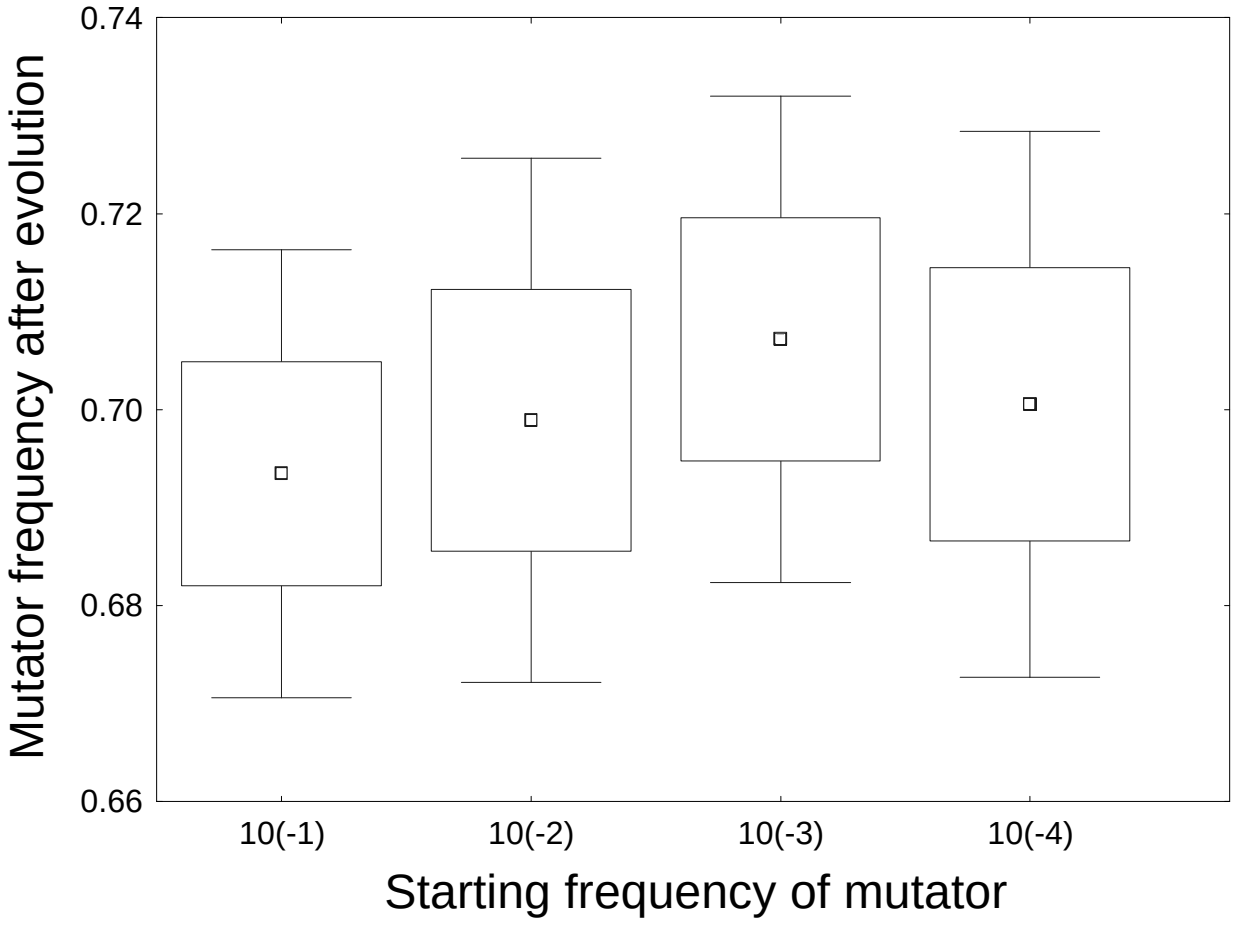

Supplementary figure 2d

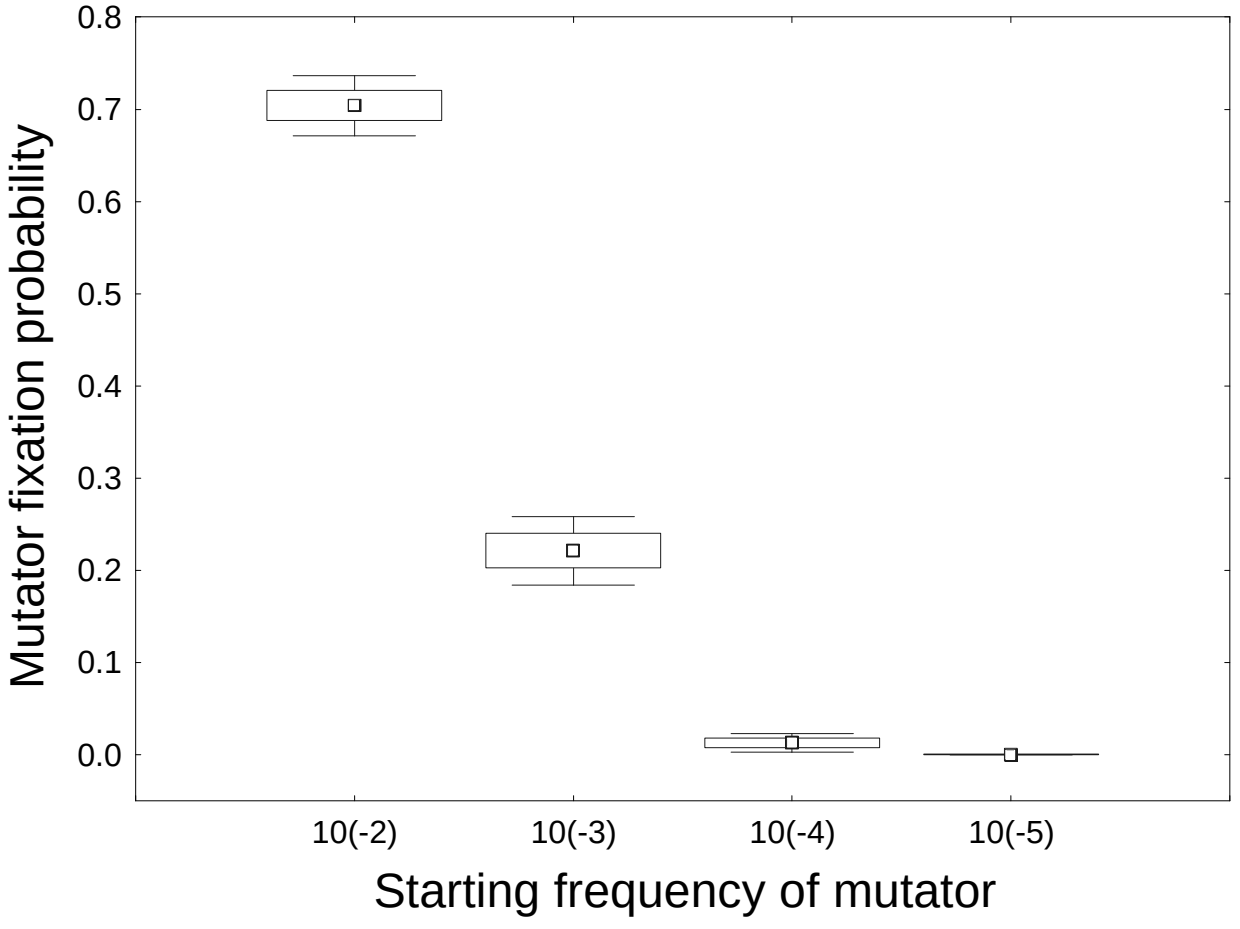

Supplementary figure 2e

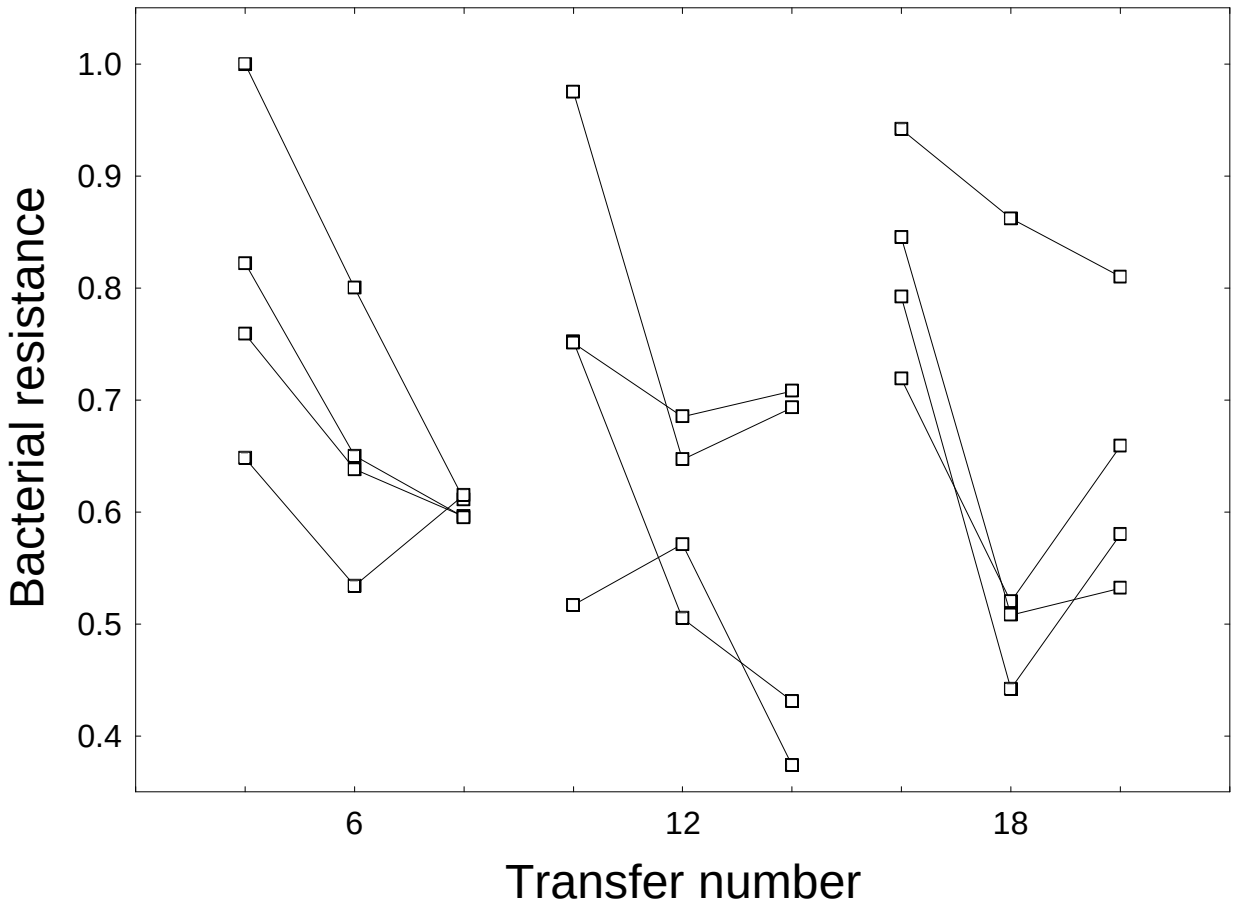

Supplementary figure 3a

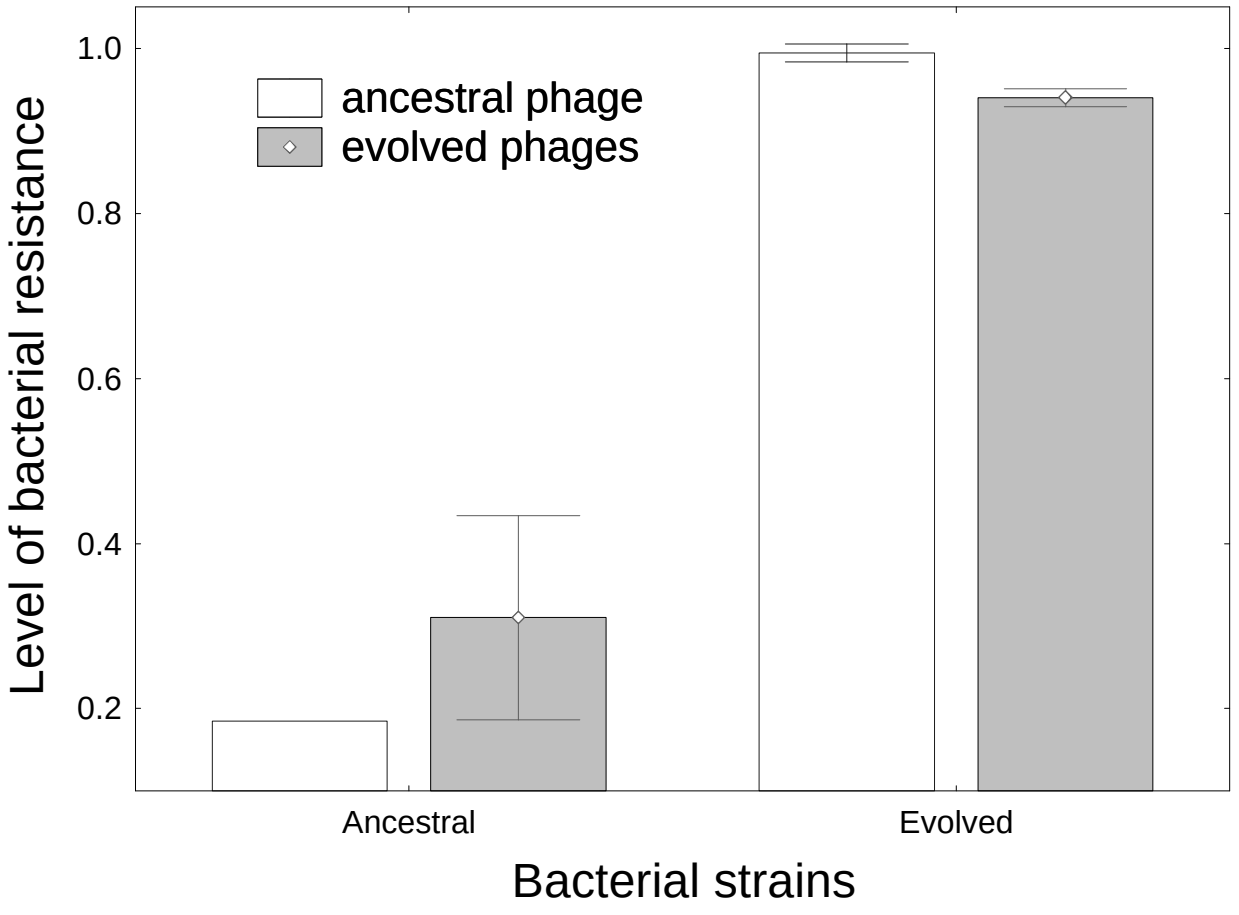

Supplementary figure 3b